Arch. Metall. Mater. **63** (2018), 1, 265-276

DOI: 10.24425/118937

L. SOZAŃSKA-JĘDRASIK*, J. MAZURKIEWICZ*, W. BOREK*#, K. MATUS*

CARBIDES ANALYSIS OF THE HIGH STRENGTH AND LOW DENSITY Fe-Mn-Al-Si STEELS

The work presents the results of investigations into the structure and phase composition of newly developed high manganese steels of the X98MnAlSiNbTi24-11 and X105MnAlSi24-11 type. The average density of such steels is 6.67 g/cm^3, which is 15% lower as compared to typical structural steels. An analysis of phase composition and structure allows to conclude that the investigated steels feature an austenitic γ-Fe(Mn,Al,C) structure with uniformly distributed and elongated α-Fe(Mn,Al) ferrite grains on the boundaries of austenite grains and carbides. Examinations by diffraction of back scattered electrons (EBSD) allow to conclude that high-angle boundaries dominate in such steels, having significant influence on mechanical properties. Three types of carbides with differentiated chemical composition and size were identified in steel X98MnAlSiNbTi24-11 with scanning and transmission electron microscopy. κ-$(Fe,Mn)_3AlC$ carbides, having a regular, face-centered cubic lattice (fcc), were identified in austenite. Transmission electron microscopy examinations have enabled to identify M_7C_3-type carbide in ferrite. Nb- and Ti-based complex carbides were identified in steel X98MnAlSiNbTi24-11, both, in ferrite and austenite. $(NbTi)C_2$ carbide precipitates were confirmed in an X-ray qualitative phase analysis. The size of the above-mentioned carbides is within several to several dozens of μm. An X-ray qualitative phase analysis has confirmed the precipitates of M_7C_3 carbides in both steels.

Keywords: high manganese steels, TRIPLEX, microstructure, isolates of carbide, carbides κ, M_7C_3, EBSD

1. Introduction

High manganese steels belong also to the group of 2nd generation high-strength AHSS steels. The are distinct for very high strength with good plasticity (Fig. 1). Some high manganese steels meet a concept of so-called light steel, due to a minimum 8% fraction of Al in chemical composition, hence the weight of structural elements is reduced [1-3]. The steels are also very often characterised by the ratio of R_p/R_m of nearly 0.9. This allows to use effectively the high values of R_m for this group of steels in structural components. Multi-faceted research has been conducted in the recent years for such steels, not only for their utilisation and for reaching high strength properties, but also for recognising the mechanisms of strengthening and correlation of structure-properties. There are also multiple technological aspects at the product forming stage, which are largely limiting a launch of this group of steels to standard production. Comprehensive information is still unavailable concerning this group of steels and occasional outcomes of research works do not allow to close them within limited frameworks in terms of properties and structure [2-4]. This work is part of research into experimental high-strength high manganese steels, whose excellent strength properties with relatively high plasticity are achieved without heat treatment already at the stage of moulding the sheets or shaped sections. Combined with the specific weight reduced in relation to typical steels, such steels allow to create structures with much smaller active sections, thus contributing not only to lower weight of the entire structure, but also to reduced material consumption; moreover, they open up new vistas for creating lightweight structures with high strength.

High manganese Fe-Mn-Al-Si steels contain 12-35% of manganese, 0-12% of aluminium, 0-3% of silicon and 0.05-1.3% of carbon. High manganese steels can be classified according to chemical composition and fall into four groups [3,4]:

- 1st group – Hadfield steel with the following concentration of chemical elements: 1.1-1.3% of C, 12-13% of Mn;
- 2nd group – steels with the following concentration of chemical elements: 0.05-0.15% of C, 15-22% of Mn, and also with a different concentration of Si and Al. A martensitic transformation is taking place in such steels as a result of cold plastic deformation (TRIP – TRansformation Induced Plasticity);
- 3rd group – steel with the following concentration of chemical elements: 0.02-0.65% of C, 20-30% of Mn, with a diverse concentration of Si and Al additives. A characteristic feature of such steels is that they possess very good plastic properties as a result of an intense curve of mechanical twinning during cold plastic deformation (TWIP effect, TWinning Induced Plasticity).
- 4th group – steels with the following concentration of chemical elements: 0.5 to 1.2% of C with a varied concentration of Mn of 18-35%, Al of 8-12% and Si of 3-6%

* SILESIAN UNIVERSITY OF TECHNOLOGY, INSTITUTE OF ENGINEERING MATERIALS AND BIOMATERIALS, 18 A KONARSKIEGO STR., 44-100 GLIWICE, POLAND

Corresponding author: wojciech.borek@polsl.pl

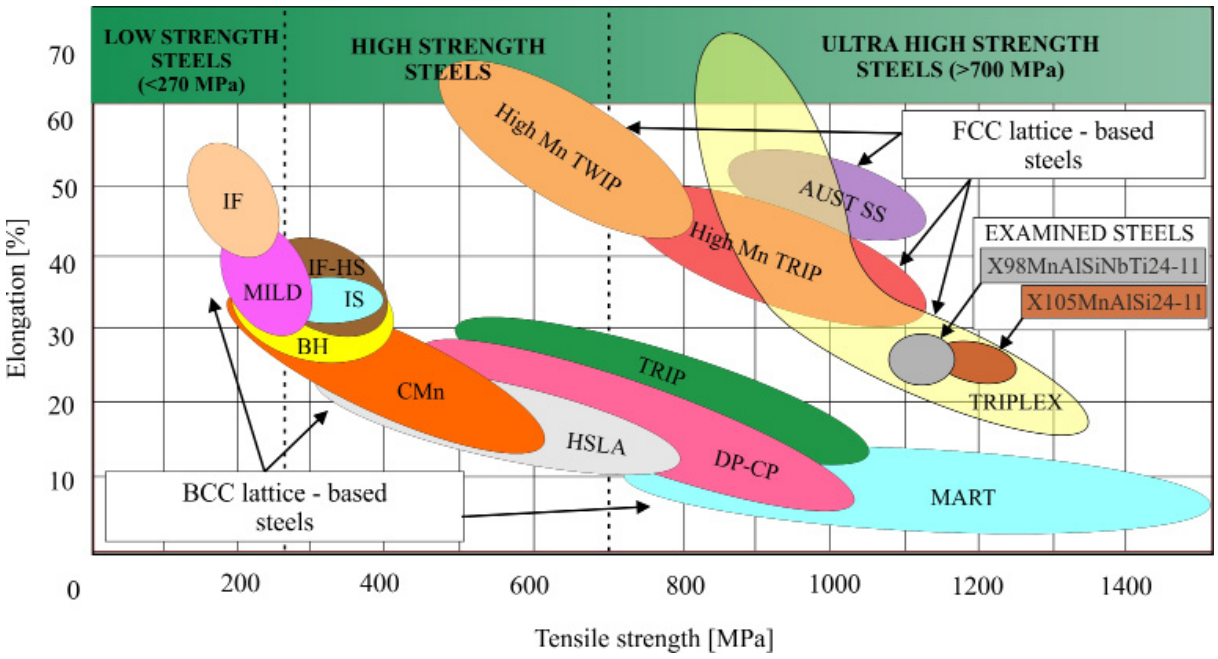

Fig. 1. Schematic representation of the mechanical properties of steel [5,11,21-40]

(Al + Si > 12%). Due to a varied fraction of dominant three phases of ferrite, austenite and dispersion precipitates of κ-(Fe,Mn)$_3$AlC carbide, the steels are called TRIPEX steels.

The studied high manganese steels presented in this work are characterised by a three-phase structure consisting of γ-Fe(Mn, Al, C) austenite, α-Fe(Mn, Al) ferrite and dispersion nanometric precipitates of κ-(Fe, Mn)$_3$AlC carbide [14]. The latest literature references for this group of steels indicate that κ-carbide, existing in such steels, has perfect stoichiometry and a crystalline structure of perovskite type. The precipitation of κ-carbides occurs as a result of spinodal decomposition [11]. The precipitation of Fe_3AlC_x carbides in Fe-Al-Mn steels may occur both, in austenite and ferrite, depending on the content of alloy elements. Mn atoms take the place of Fe atoms in Fe-Al-Mn-C alloys, and stoichiometry of Fe_3AlC_x carbide is transformed into (Fe, Mn)$_3$AlC$_x$ (Fig. 2) [13]. κ-carbides are characterised by a regular, face-centred cubic lattice (fcc) with the E21 perovskite structure [20]. Mechanical properties of high manganese steels are largely dictated by the location, size and morphology of κ-(Fe, Mn)$_3$AlC$_x$ carbides. Such carbides may also be a reason for steel brittleness during plastic deformation at room temperature, when they form large precipitates on grain boundaries [10-12]. The location and morphology of κ carbide has a considerable effect on steel elongation and strength [6-8]. Stacking faults between κ-carbides and austenite (γ) can be controlled by adding niobium and titanium, and stacking-fault energy (EBU ~ 110 mJ/m^2) may lead to manifestation of the SIP effect -– Shear Band Induced Plasticity [9]. The SIP effect is the main strengthening mechanism of TRIPLEX high manganese steel, where intersecting shear bands are created in austenite. Shear bands, together with uniformly arranged carbides exhibiting coherence with the matrix, impede the dislocation movements. The result of this effect is a high rate of strain hardening during stretching, which prevents a neck from being formed too fast in a specimen, to value of high yielding R_p/R_m [14,41-44].

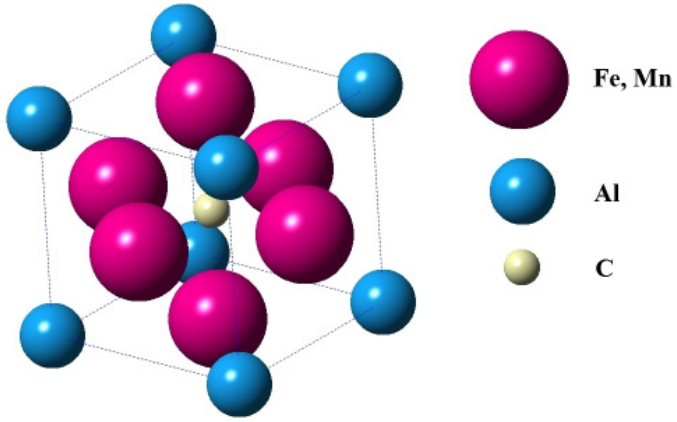

Fig. 2. Unit cell of κ-carbide [8]

2. Experimental (materials and methods)

The aim of the work was to identify a structure and phases of the newly developed high manganese X98MnAlSiNbTi24-11 and X105MnAlSi24-11 type steels of the TRIPLEX type in the input state for final hot plastic working.

Two high manganese steels were investigated (Tab. 1): steel X98MnAlSiNbTi24-11 with microadditives of Ti and Nb, and the other steel X105MnAlSi24-11 without microadditives.

The studied steel was melted in a laboratory vacuum induction furnace of the VSG-50 type produced by Balzers. The steels were cast into an ingot mould in the atmosphere of argon. The hot plastic working of the ingot was performed after cooling in

TABLE 1

The chemical compositions of the examined steels

Elements	C	Mn	Al	Si	Nb	Ti	Ce	La	Nd	P_{max}	S_{max}
Steel X98MnAlNbTi24-11											
[wt. %]	0.98	23.83	10.76	0.20	0.048	0.019	0.029	0.006	0.018	0.002	0.002
Steel X105MnAlSi24-11											
[wt. %]	1.05	23.83	10.76	0.10	—	—	0.037	0.011	0.015	0.005	0.005

the air, with open die forging using a high-speed hydraulic press with the pressure of 300 tonnes. Forging temperature ranged between 1200 and 900°C with reheating between operations so that the material temperature was not below 900°C. 32 mm thick and 200 mm wide section-shaped test specimens were cut out from the material after forging for examinations.

The structure of the investigated steel was observed with a light microscope (LM), pictures of the structures of our investigated steels have been taken with the magnifications of 100-1000x. The specimens for structural examinations in an electron scanning microscope were embedded, then ground and polished mechanically with sandpapers and discs wetted with a diamond suspension. A 5% HNO_3 solution in ethyl alcohol (nital) was used as a reagent to reveal the structure. The etching time was about 10-70 s. The specimens for diffraction examinations by EBSD technique in a scanning electron microscope were ground with a grinder-polisher with sandpapers and then polished electrochemically in a reagent with the following composition:

- 950 ml of 99% hydrochloric acid (CH_3COOH);
- 50 ml of 60% tetraoxochloric acid ($HClO_4$).

The observations of the investigated steels' microstructure were performed in a scanning and transmission electron microscope. Examinations in a scanning electron microscope, Zeiss Supra 35, were carried out at the accelerating voltage of 5 to 20 kV using secondary electrons (SE) detection. The images of the examined steels' structures were made with a magnification of 50-120,000×. The EDS Edax TRIDENT XM4 detector was used to determine the qualitative and quantitative chemical composition of the microareas of the examined steels and precipitates. Examinations by diffraction of back scattered electrons (EBSD) were made with the accelerating voltage of 20 kV, working distance of 15 mm and step size of 0.20 µm.

The isolates of carbide phases were made to identify the released carbides in the examined steels. Carbide isolates were made by dissolving a matrix of steel specimens as a result of anodic stripping. Fig. 3 presents a diagram of a station for anodic stripping. The suspensions produced were decanted with distilled water and final rinsing was performed using ethyl alcohol. The produced suspension was filtrated with Nalgene PS Filter Holder and Receiver 250. The sediment was left to dry.

An X-ray qualitative phase analysis was carried out with an X-ray X'Pert PRO diffraction metre by PANalytical equipped with a band detector, PIXcel^{3D} to identify the carbides from carbide isolates. The parameters of X-ray examinations are shown in Table 2.

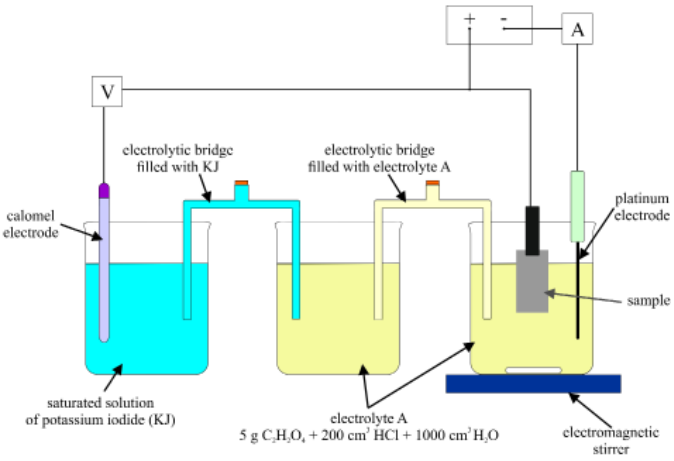

Fig. 3. Scheme anodic dissolution [18]

TABLE 2

Parameters of X-Ray diffraction examinations

Parameters of examinations	Carbide isolates
angular range	40-120°
step size	0.026°
scan step time	197 s
lamp	cobalt, λ = 1.78901 Å
tension	40 kV
current	30 mA

The samples for structural examinations in transmission electron microscope (TEM) have been cut, then TEM samples were prepared by mechanical grinding the specimens to a thickness of 60 µm and ion beam polishing. Transmission electron microscope studies were conducted at the accelerating voltage of 300 kV. TEM investigations were performed in a probe Cs-corrected S/TEM Titan 80-300 FEI microscope equipped with EDAX EDS. Selected area electron diffraction patters were obtained with camera length of 215 and condenser aperture C2-50. In STEM mode HAADF (high angle annular dark field) was used with convergence angle of 24 mrad.

3. Results and discussion

The steels X98MnAlSiNbTi24-11 and X105MnAlSi24-11 are characterised by an austenitic-ferritic structure with precipitates of carbides with a diverse composition and morphology (Figs. 4,5), which was confirmed through examinations with a scanning and transmission electron microscope. It was

found that ferrite grains in the examined TRIPLEX steels are elongated and distributed uniformly along the boundaries of austenite grains. Ferritic areas in steel X105MnAlSi24-11 along the boundaries of austenite grains are larger than in case of steel X98MnAlSiNbTi24-11 due to a fraction of Nb and Ti in the chemical composition of the latter of the mentioned steels. Small ferritic areas inside austenite grains can be observed in both steels (Fig. 4c, Fig. 5c). It can be confirmed by analysing the results of steel examinations that austenite grains in steel

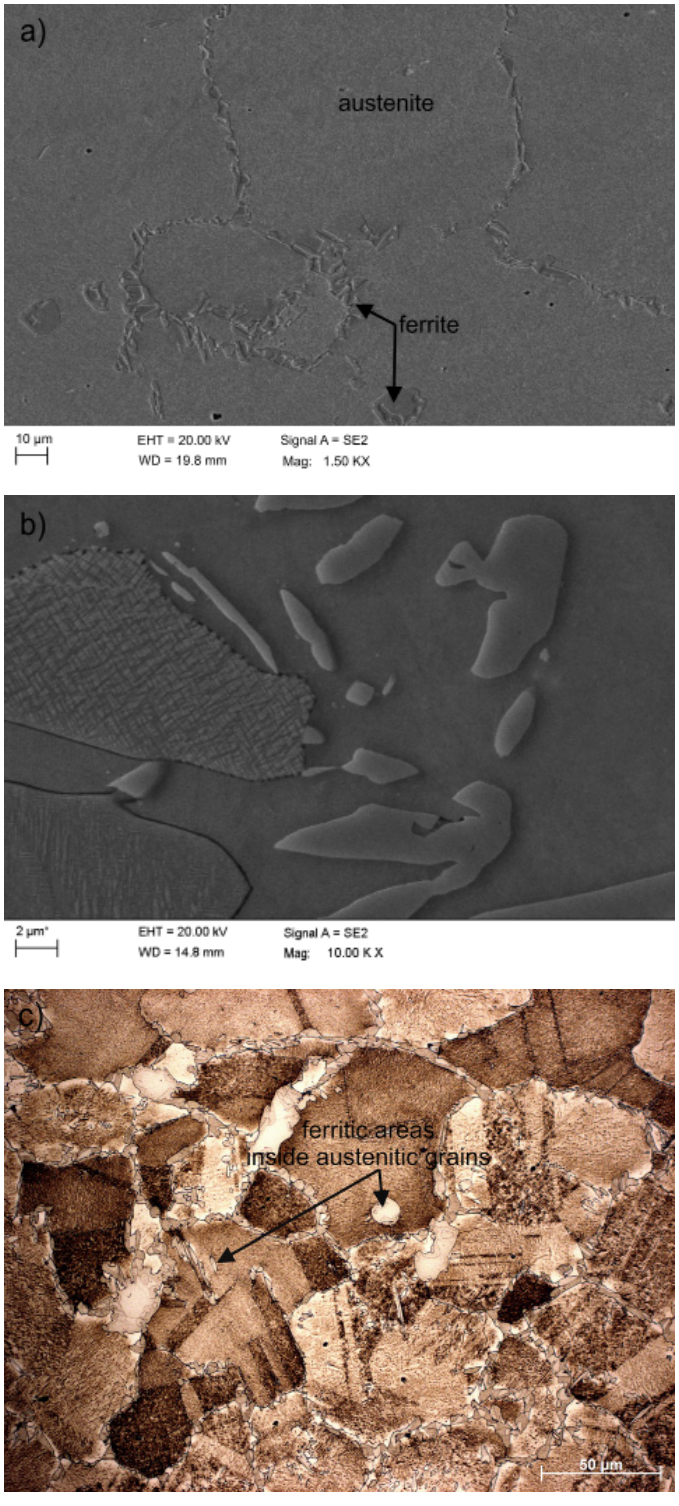

Fig. 4. Austenitic-ferritic microstructures of high manganese X98MnAlSiNbTi24-11 steel: a), b) SEM image; c) LM image

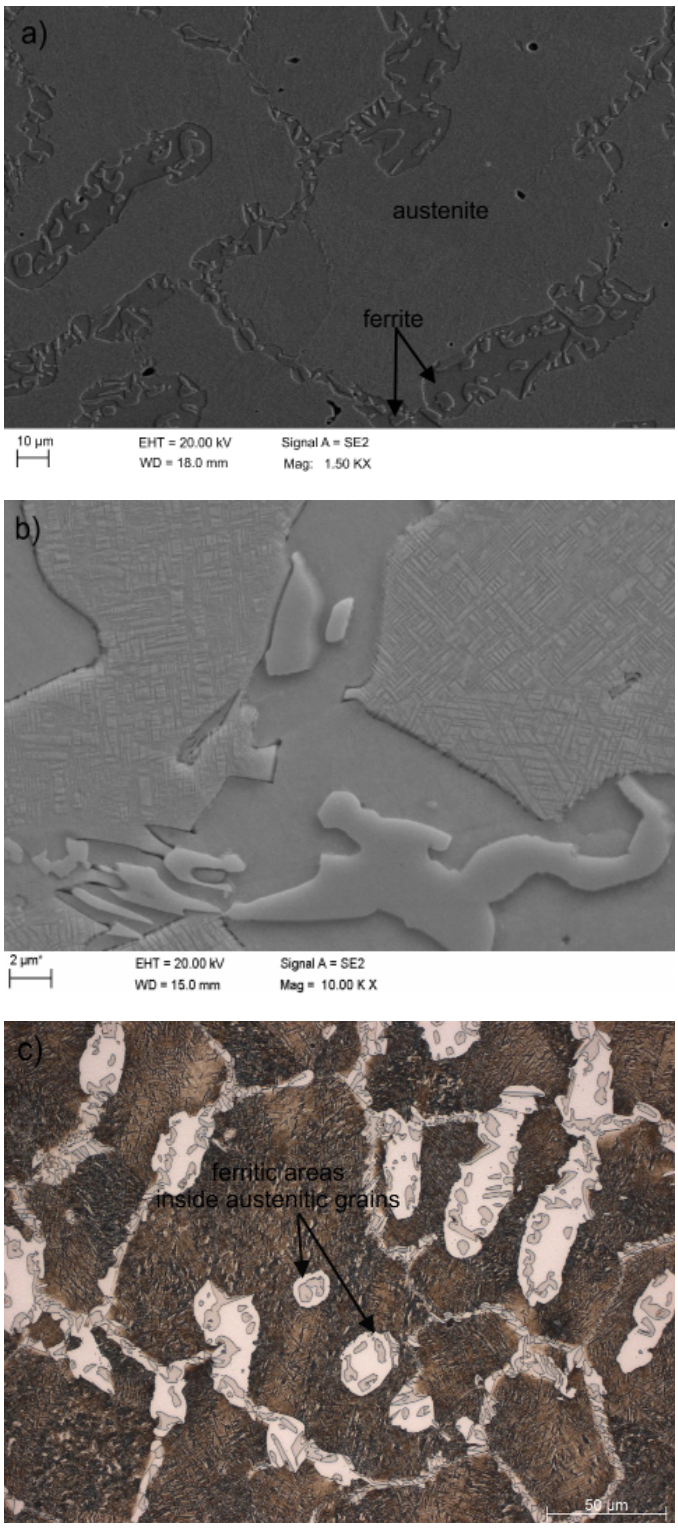

Fig. 5. Austenitic-ferritic microstructures of high manganese X105MnAlSi24-11 steel: a), b) SEM image; c) LM image

with Nb and Ti are also smaller than for steel without such additives. It can be concluded by comparing steel structures that micro-additives of Nb and Ti influence grain refinement, as confirmed by literature reports for other high manganese steels [15-17].

The investigations of carbides isolated from the matrix of steel X98MnAlSiNbTi24-11 give a more complete picture of

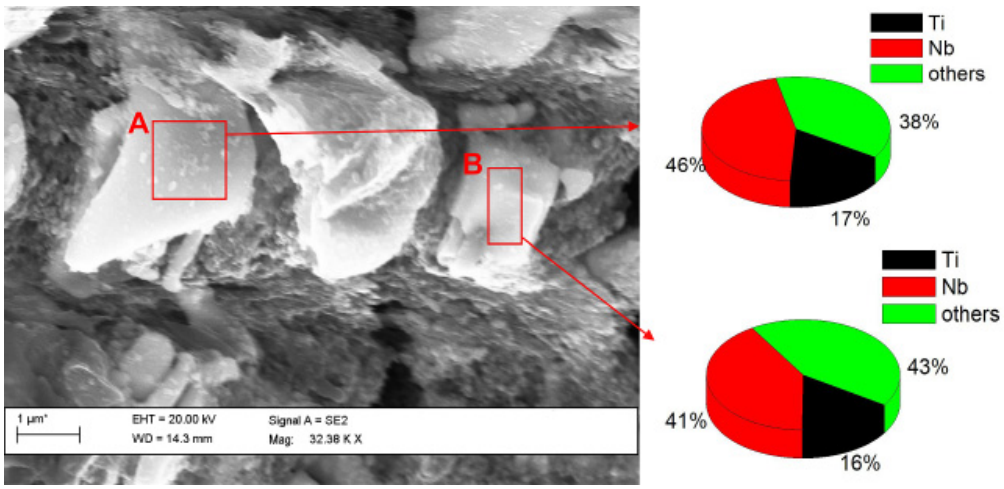

Fig. 6. Carbides isolated from X98MnAlSiNbTi24-11 steel matrix with chemical composition measurement by EDS in the indicated microareas (SEM)

their morphology, size and chemical composition, as well as a fraction volume. Fig. 6 shows carbides isolated from a matrix; it was concluded based on a chemical composition examination that these are complex carbides, whose composition is based, most of all, on Ti and Nb. The morphology and size of such carbides is highly varied, spanning between several nanometres to even several dozens of µm [14,32]. A small fraction of oxygen and aluminium represents probably the residues of matrix dissolution processes. Interesting results were obtained by analysing the smallest isolated carbides extracted from a homogenised ether solution on platinum sputtered glass and on the polished pure copper (Fig. 7). Such carbides have a regular cubical shape, with the size of carbides – that were managed to be measured – of between several to 160 nm.

Fig. 8 and Fig. 9 present the results of examinations of structure using EBSD techniques in SEM. The examinations,

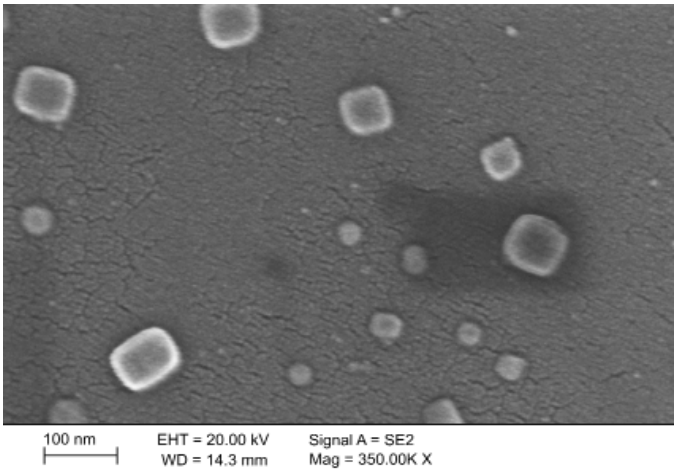

Fig. 7. Dispersive carbides isolated from X98MnAlSiNbTi24-11 steel matrix on glass plate (SEM)

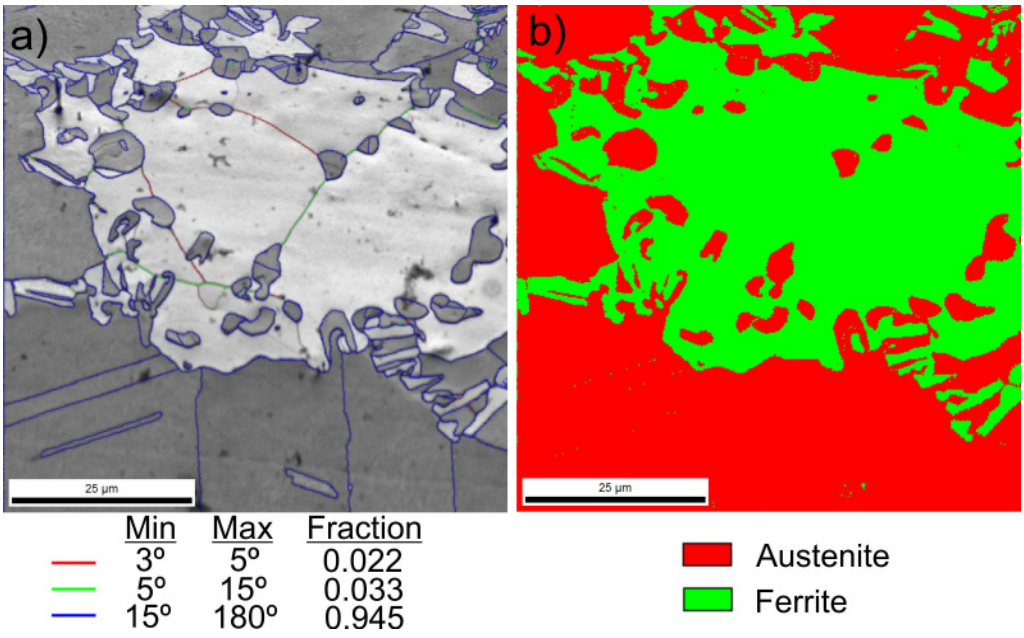

Fig. 8. Structure revealed by EBSD technique in SEM in the selected microarea of the investigated X98MnAlSiNbTi24-11 steel, a) IQ map with highlighted misorientation angles, b) EBSD phase map

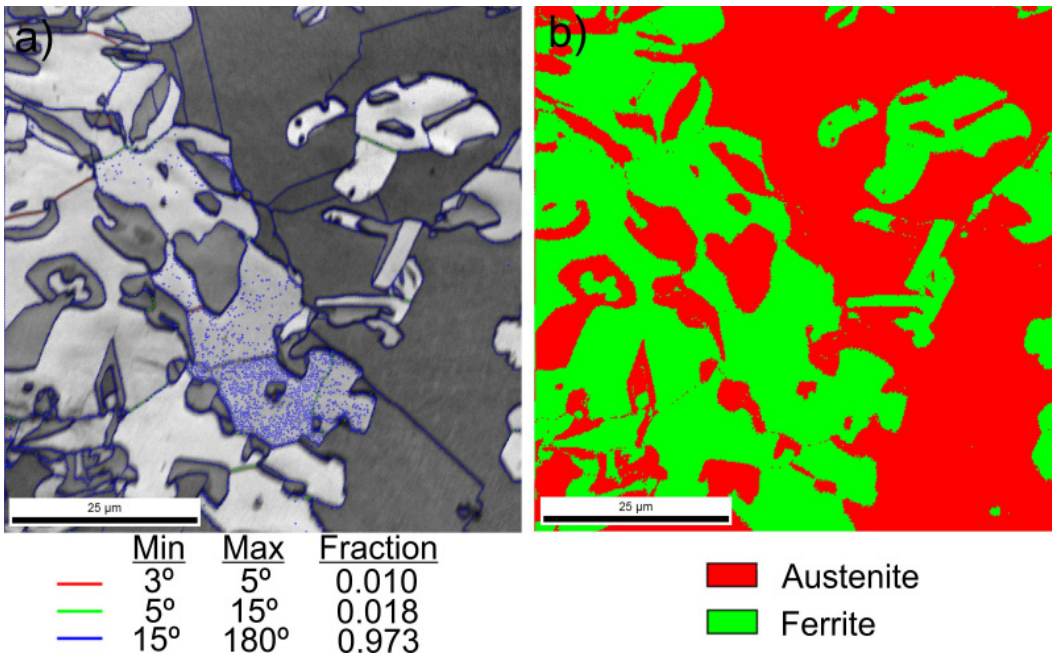

Fig. 9. Structure revealed by EBSD technique in SEM in the selected microarea of the investigated X105MnAlSi24-11 steel, a) IQ map with highlighted misorientation angles, b) EBSD phase map

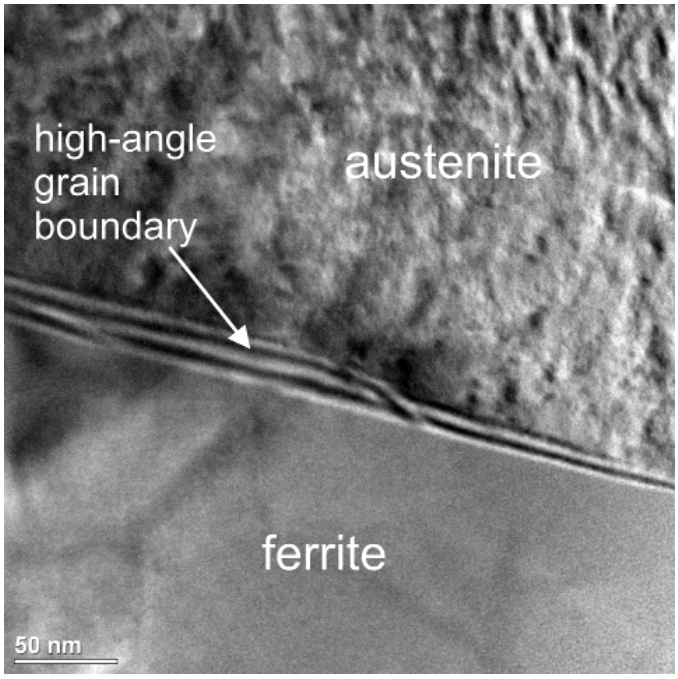

Fig. 10. TEM image of the X98MnAlSiNbTi24-11 steel

performed with EBSD, allow to confirm the distribution and location of the particular structure components together with their morphology and size. It can be claimed based on EBSD examinations that high-angle boundaries dominate in both steels (misorientation angle ≥15°) (Fig. 8a, Fig. 9a). High-angle boundaries are not flat surfaces, but contain blisters or faults, so-called protrusions [21], as noticed in Fig. 4a, Fig. 5a and Fig. 10. Microareas with a higher content of Al and Mn, but smaller content of Fe, were found based on distribution maps of chemical elements, which may indicate that the above-mentioned revealed phases with a similar structure, but differentiated composition in an elementary cell, may exist in such places. Microareas with a higher content of Nb and Ti were noticed in steel X98MnAlSiNbTi24-11. It was found based on distribution maps of chemical elements (Fig. 6, Fig. 10) that these are mainly complex carbides based on Nb and Ti.

Figure 10 shows an austenitic-ferritic microstructre of Steel X98MnAlSiNbTi24-11. A fault on a high-angle boundary of austenite and ferrite grains was also noticed [21]. TEM examinations of steel X98MnAlSiNbTi24-11 showed that Nb- and Ti-based dispersive carbides are precipitated both, in austenite and ferrite (Fig. 11, Fig. 12). Apart from the above-mentioned carbides with Nb and Ti, two types of carbides were also identified: M_7C_3 carbide and κ-carbide. κ-carbide was identified in austenite of the studied steel (especially with the band axis [211] Fig. 13, Fig. 14), having a regular, wall-centred lattice (fcc) (Pm-3m group) with a lattice parameter of a = 0.3875 nm. A lattice parameter is slightly higher than described in publications for this group of steels [19]. M_7C_3-type carbide was identified in ferrite of steel X98MnAlSiNbTi24-11 (Fig. 15 with the band axis [192]). M_7C_3-type carbide features an orthorhombic crystalline lattice (Pnma group) with lattice parameters a = 0.4546 nm, b = 0.6959 nm, c = 1.197 nm. Ferrite (Fig. 16) and austenite (Fig. 17), and also κ-carbide were identified in steel B.

X-ray examinations of carbides isolated from a matrix of steel specimens as a result of anodic stripping (Fig. 18, 19) have confirmed the existence of M_7C_3 carbides in both examined steels, while $(NbTi)C_2$-type carbides were additionally identified in steel X98MnAlSiNbTi24-11. κ-carbides, identified in transmission electron microscope examinations, were not discovered by a diffractometer due to the fraction below the test method's detectability threshold.

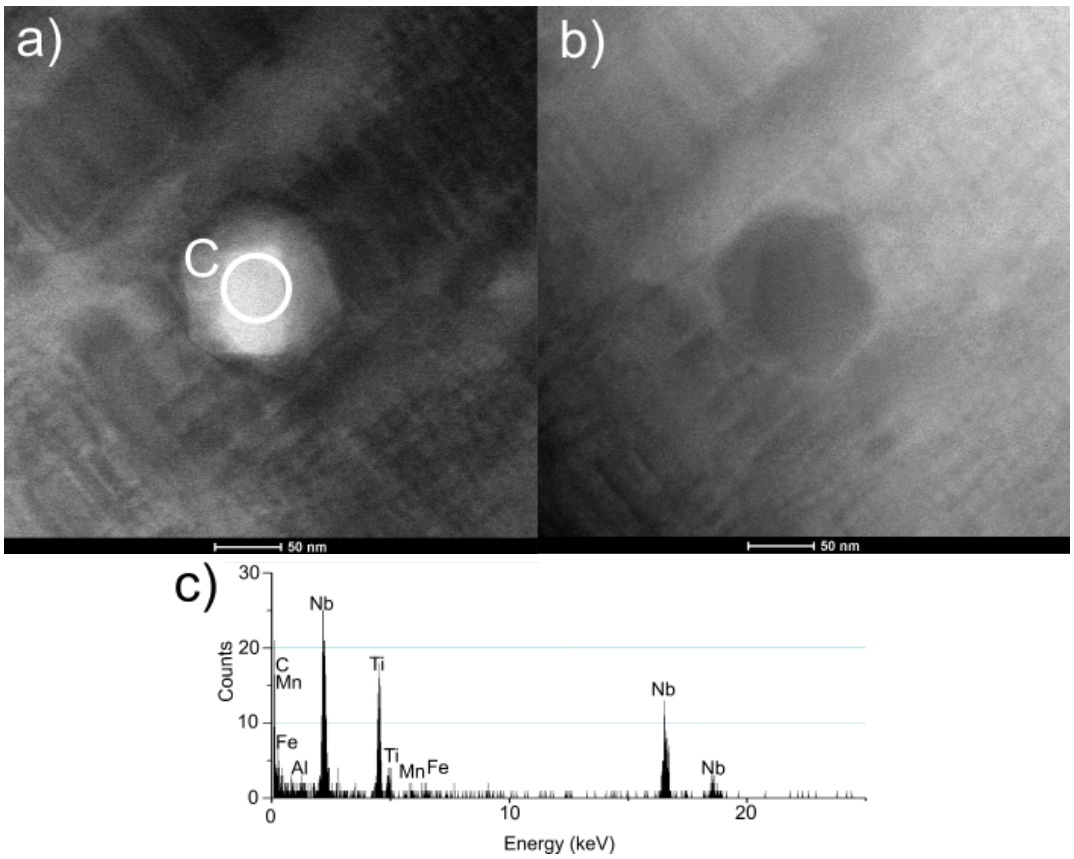

Fig. 11. Precipitation based on Nb and Ti in the austenite – X98MnAlSiNbTi24-11 steel: a) dark-field image, b) bright field image, c) EDS spectrum from the area C

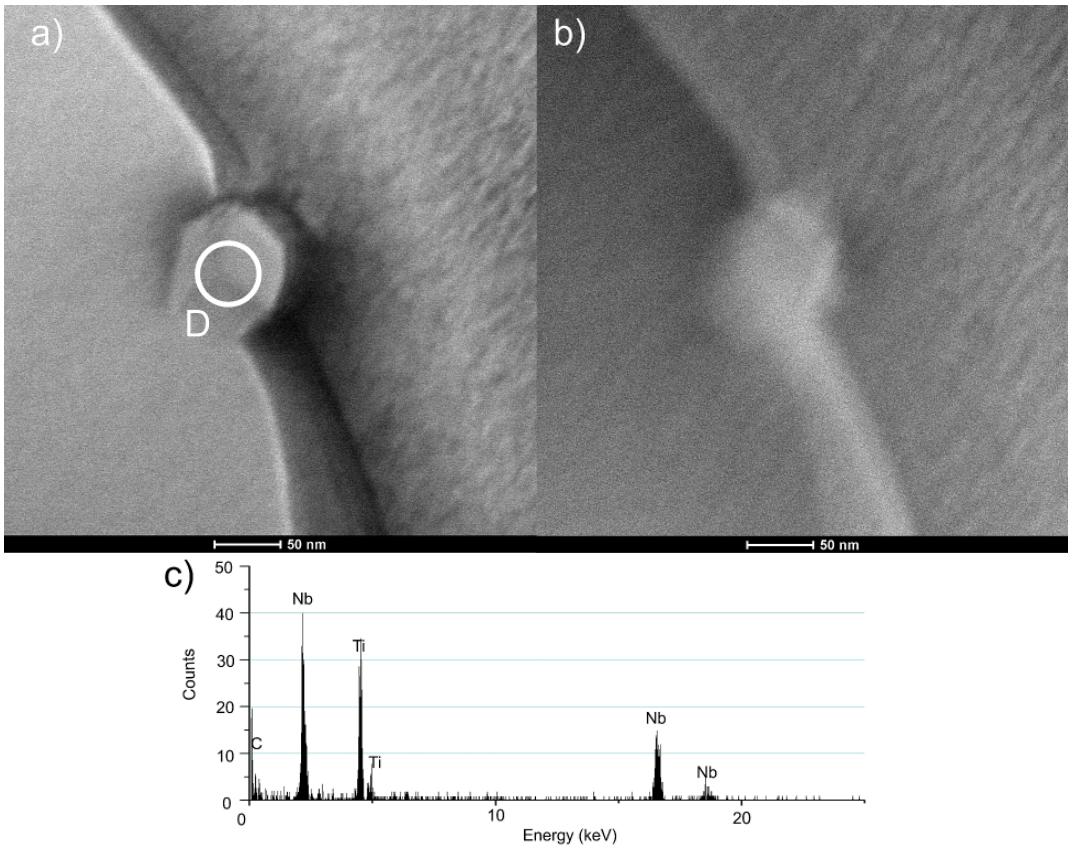

Fig. 12. Precipitation based on Nb and Ti in the ferrite – X98MnAlSiNbTi24-11 steel: a) dark-field image, b) bright field image, c) EDS spectrum from the area D

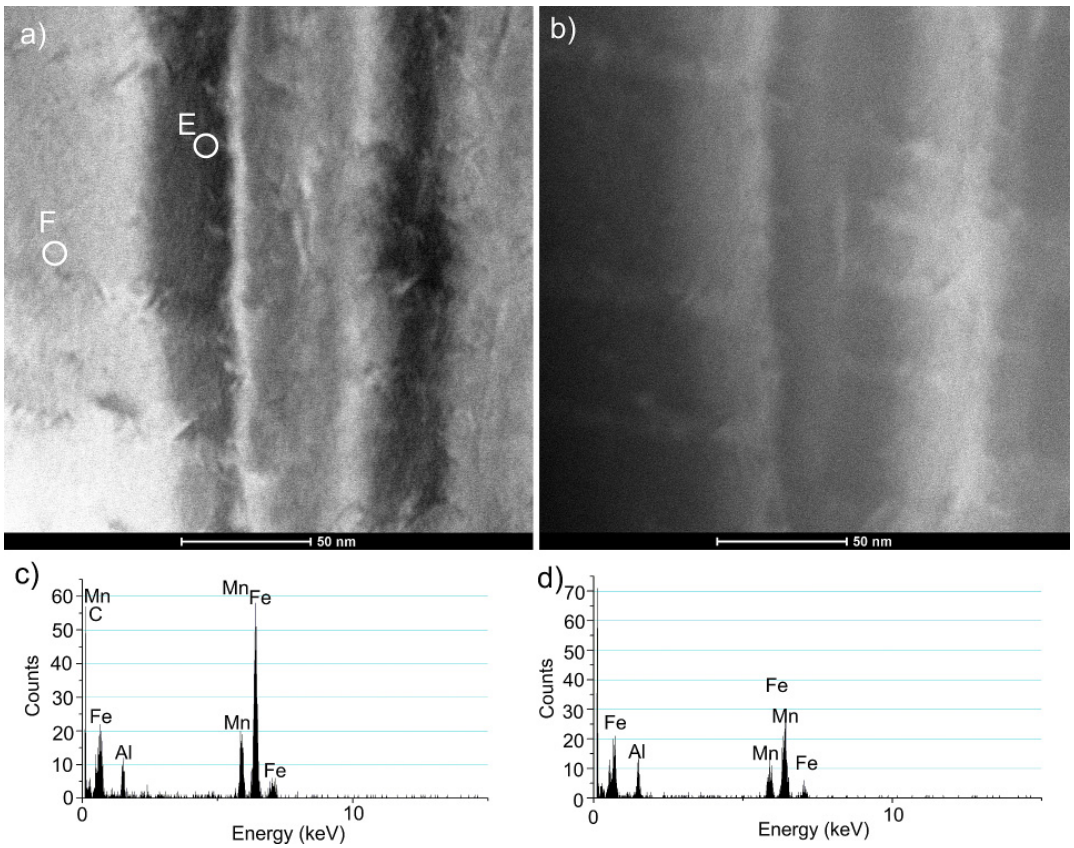

Fig. 13. Precipitation κ carbide in austenite – X98MnAlSiNbTi24-11 steel a) dark-field image, b) bright field image, c) EDS spectrum from the area E, d) EDS spectrum from the area F

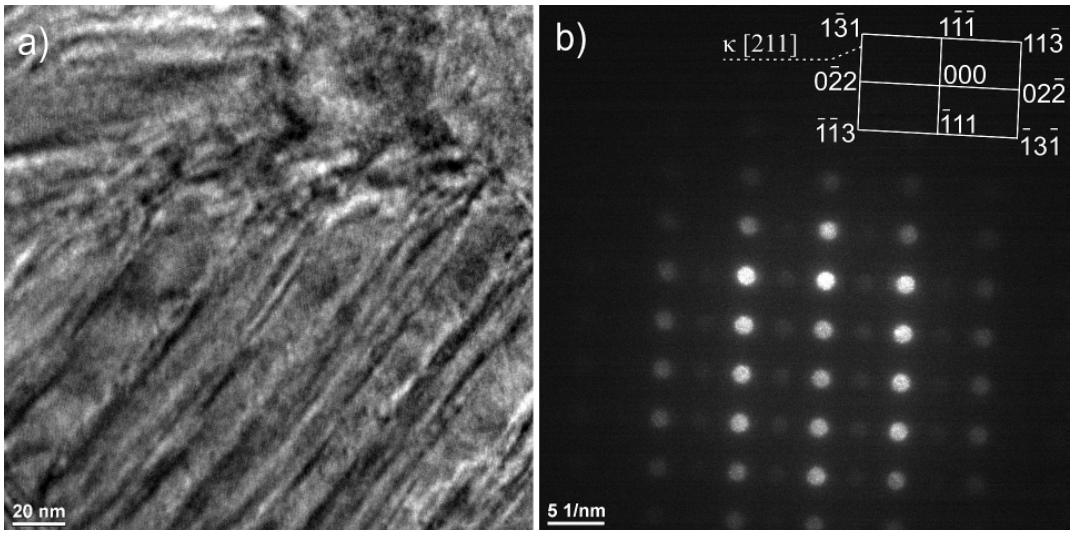

Fig. 14. TEM image of the X98MnAlSiNbTi24-11 steel a) precipitates in austenite, b) diffraction pattern of the zone axis [211] κ

4. Conclusion

The following conclusions were drawn based on the outcomes of the investigations and according to their analysis:

- A structure of the investigated, newly created TRIPLEX steels in the input state for final hot plastic working consists of austenite, ferrite and carbides. Ferritic areas are uniformly distributed on the boundaries of austenite grains. Small ferritic areas exist inside austenite grains. The results of chemical composition examinations in microareas using EBSD technique in a scanning electron microscope have confirmed the above-mentioned phase composition of the studied steel.
- It was found based on EBSD examinations that high-angle boundaries with faults existing on them dominate in both steels (misorientation angle ≥15°).
- The examinations carried out using scanning and transmission electron microscopy of steel X98MnAlSiNbTi24-11

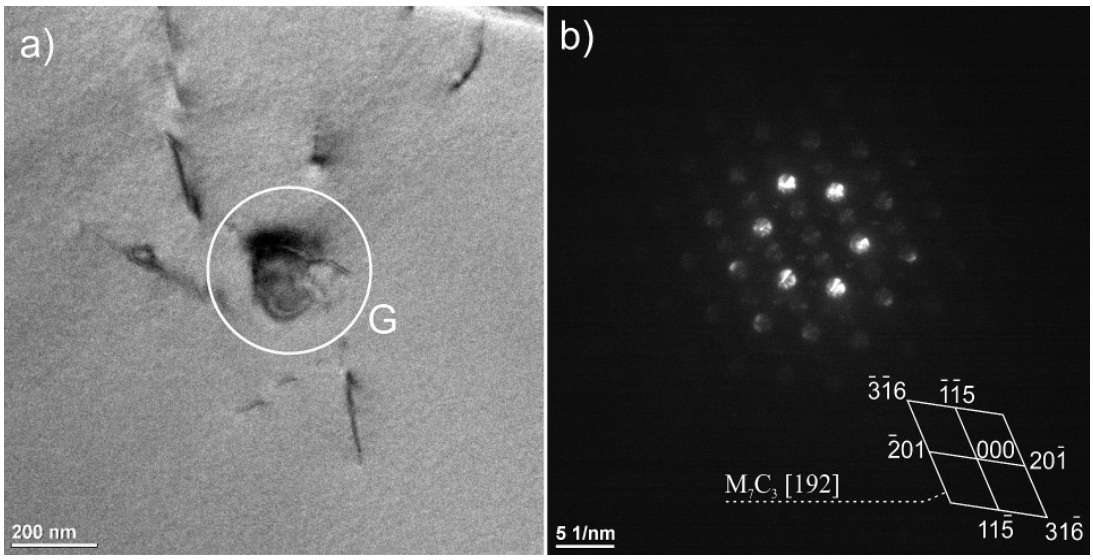

Fig. 15. TEM image of the X98MnAlSiNbTi24-11 steel, a) precipitates in ferrite, b) diffraction pattern of the zone axis [192] M_7C_3

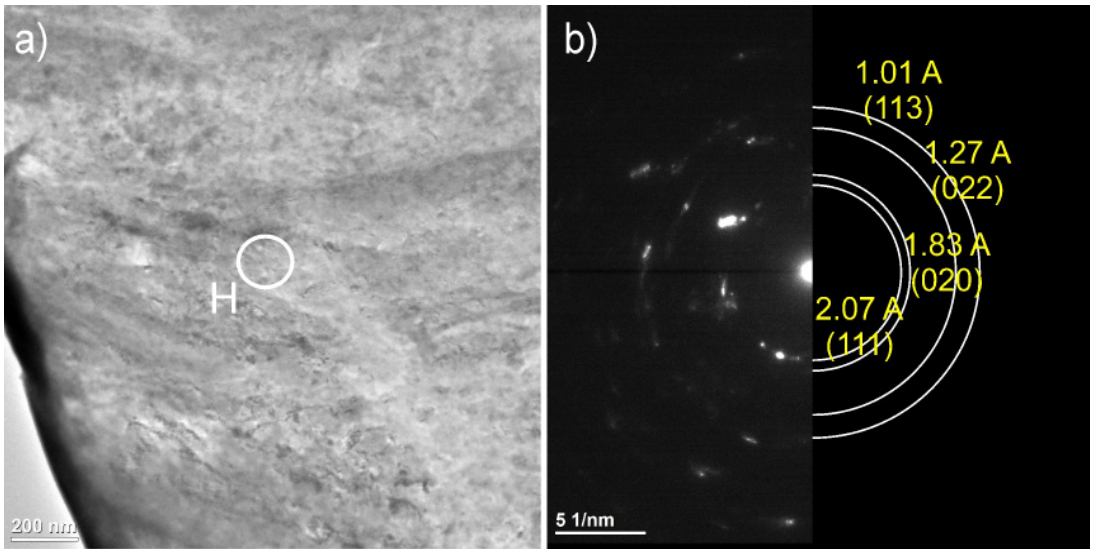

Fig. 16. a) TEM image of the X105MnAlSi24-11 steel, b) diffraction pattern of ferrite α-Fe(Mn, Al)

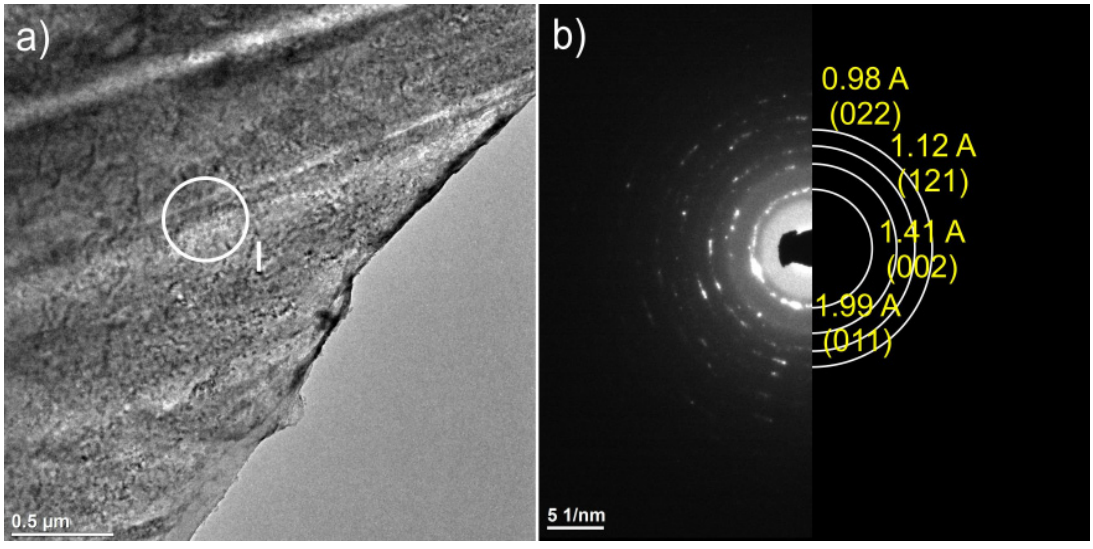

Fig. 17. a) TEM image of the X105MnAlSi24-11 steel, b) diffraction pattern of austenite γ-Fe(Mn, Al, C)

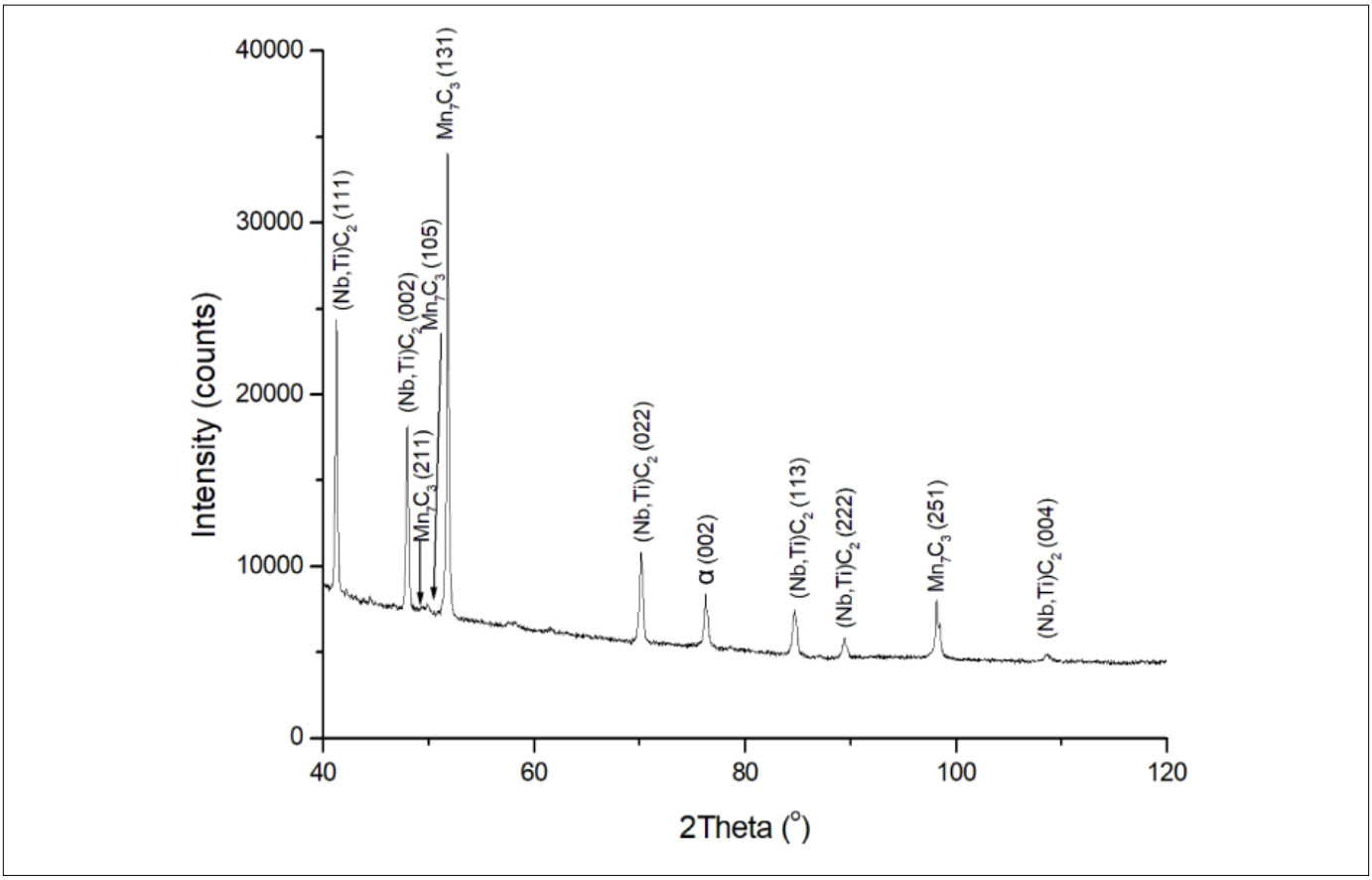

Fig. 18. X-ray diffraction pattern of carbides isolated from X98MnAlSiNbTi24-11 steel

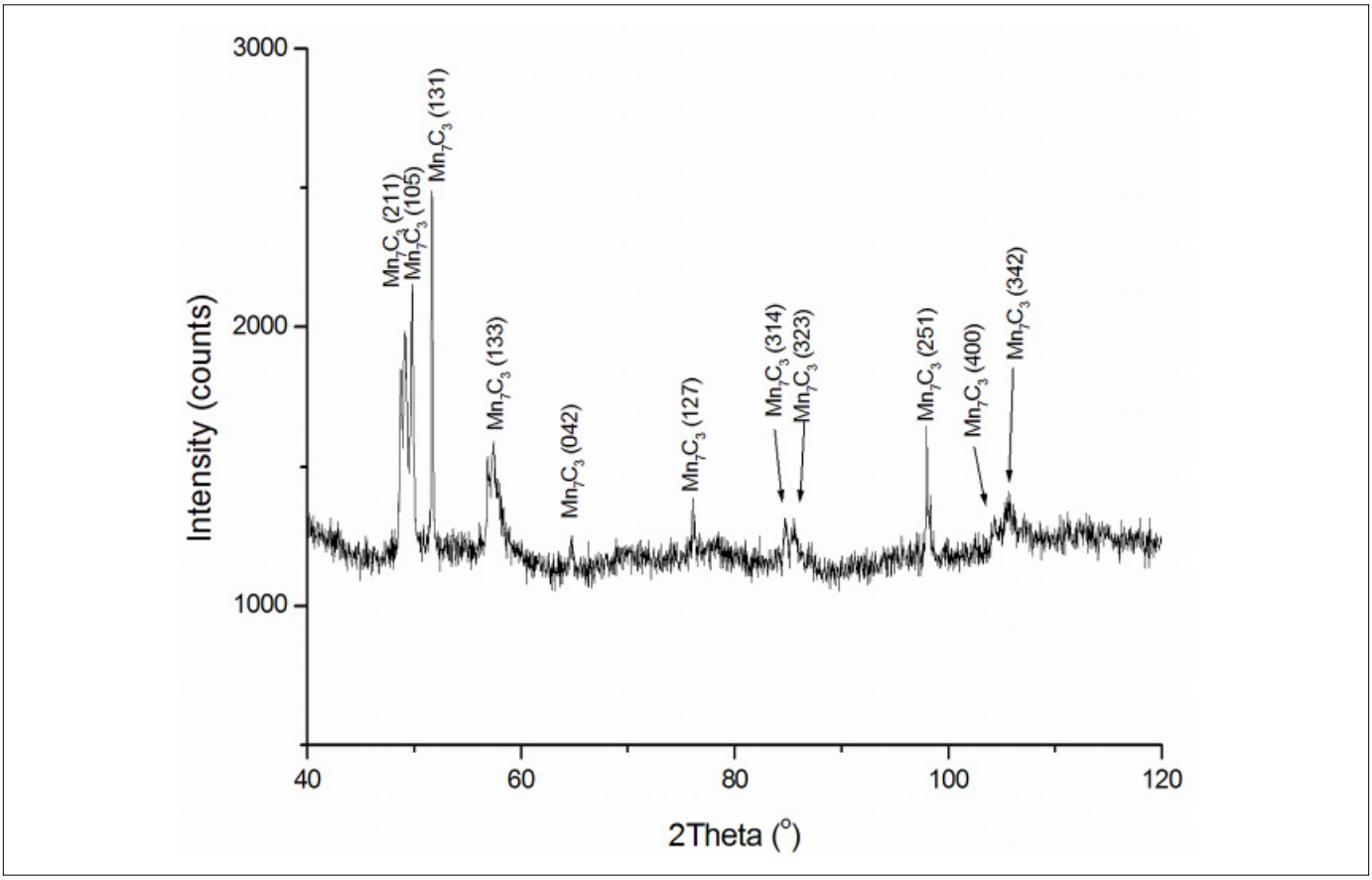

Fig. 19. X-ray diffraction pattern of carbides isolated from X105MnAlSi24-11 steel

have revealed that Nb- and Ti-based complex carbides existed in ferrite and austenite. The size of the above-mentioned carbides is within several to several dozens of μm. It can be pointed out by comparing the steel structure of both steels that micro-additives of Nb and Ti influence grain refinement.

- The examinations of the structure of steel X98MnAlSiNbTi24-11 in a transmission electron microscope have allowed to identify Nb- and Ti-based complex carbides, M_7C_3 carbides and κ-carbides. κ-carbide was revealed in austenite grains with a regular crystalline lattice, and M_7C_3 carbide in ferrite grains having an orthorhombic crystalline lattice.
- M_7C_3 carbides were identified on X-ray diffraction patterns of both steels from the obtained carbide isolates. Complex $(NbTi)C_2$ carbides were identified in steel with Nb and Ti micro-additives.

The examinations of the structure and phase composition of steel X98MnAlSiNbTi24-11 and X105MnAlSi24-11 of the TRIPLEX type, the results of which are presented in this work, are a starting point for analysing structural changes of such steels during technological procedures aimed at achieving the final usable form, resulting in reaching the specific strength properties. The results of investigations showing how hot plastic working influences changes in properties and structure of analysed steels will be presented in the team's next works. This will also allow to better recognise and analyse strengthening mechanisms of such steels, and examinations with a plastic deformation simulator, Gleeble 3800, will also serve this. Apart from typical parameters determined for high-strength steels, it is also important to recognise corrosion resistance of this group of materials, especially considering stress corrosion and its impact resistance, which is now being analysed and will soon be published.

Acknowledgements

Scientific work was financed in the framework of project funded by the National Science Centre based on the decision number DEC-2012/05/B/ST8/00149.

Liwia Sozańska-Jędrasik is a scholarship holder of the Visegrad International Scholarship Grant for the period September 2017 to June 2018, so some of the research was conducted in collaboration with Ing. Martin Kraus from VŠB – Technical University of Ostrava in the Czech Republic.

REFERENCES

[1] M. Jabłońska, Hutnik – Wiadomości Hutnicze **6** (81), 385-389 (2014).
[2] A. Grajcar, Stal Met. Nowe Technol. **7/8**, 10-13 (2013).
[3] N. Cabañas, N. Akdut, J. Penning, B.C. De Cooman, Metall. Mater. Trans. A **37**/11, 3305-3315 (2006).
[4] M. Witkowska, A. Zielinska-Lipiec, J. Kowalsk, W. Ratuszek, Arch Metall Mater **59**, 3, 971-975 (2014).
[5] A. Grajcar, P. Skrzypczyk, R. Kuziak, K. Gołombek, Steel Res. Int. **85** (6), 1058-1069 (2014).
[6] X. Tian, H. Li, Y. Zhang, J. Mater. Sci. **43** (18), 6214-6222 (2008).
[7] Y. Kimura, K. Handa, K. Hayashi, Y. Mishima, Intermetallics **12** (6), 607-617 (2004).
[8] Y. Kimura, K. Hayashi, K. Handa, Y. Mishima, Mat. Sci. Eng. A-Struct. **329**, 680-685 (2002).
[9] G. Frommeyer, U. Brüx, Steel Res. Int. **77** (9-10), 627-633 (2006).
[10] E. Mazancová, Z. Jonšta, K. Mazanec, Hutnické listy **2**, 60-63 (2008).
[11] M. Bausch, G. Frommeyer, H. Hofmann, E. Balichev, M. Soler, M. Didier, L. Samek, Ultra high-strength and ductile FeMnAlC light-weight steels (MnAl-steel), Luxembourg 2013.
[12] I. Gutierrez-Urrutia, D. Raabe, Mater Sci. Tech. Ser. **30**, 9, 1099-1104 (2014).
[13] V. Rigaud, D. Daloz, J. Drillet, A. Perlade, P. Maugis, G. Lesoult, ISIJ INT **47**, 6, 898-906 (2007).
[14] L.A. Dobrzański, W. Borek, Mater. Sci. Forum. **654-656**, 266-269 (2010).
[15] S.S. Sohn, H. Song, B.C. Suh, J.C. Suh, J.H. Kwak, B.J. Lee, N.J. Kim, S. Lee, Acta Mater. **96**, 301-310 (2015).
[16] K. Eipper, G. Frommeyer, W. Fussnegger, A. Gerick, W. Kleineathoefer, United States Patent Application Publication US 2007/0125454A1 (2007).
[17] M.C. Ha, Mat. Sci. Eng. A-Struct. **586**, 276-283 (2013).
[18] R. Chylińska, B. Piekarski, Archiwum Technologii Maszyn i Automatyzacji **27**, 1, 113-120 (2007).
[19] C.-Y. Chao, C.-H. Liu, Mater Trans. **43**, 10, 2635-2642 (2002).
[20] L.N. Bartlett, D.C. van Aken, J. Medvedeva, D. Isheim, N.I. Medvedeva, K. Song, Metall. Mater. Trans. A **45**, 2421-2435 (2014).
[21] F. Yang, R. Song, Y. Li, T. Sun, K. Wang, Materials and Design **76**, 32-39 (2015).
[22] M. Koyama, H. Springer, S.V. Merzlikin, K. Tsuzaki, E. Akiyama, D. Raabe, Int. J. Hydrogen. Energ. **39**, 4634-4646 (2014).
[23] L. Zhang, R. Song, C. Zhao, F. Yang, Y. Xu, S. Peng, Mat. Sci. Eng. A-Struct. **643**, 183-193 (2015).
[24] H. Springer, D. Raabe, Acta Mater. **60**, 4950-4959 (2012).
[25] D. Kuc, E. Hadasik, G. Niewielski, I. Schindler, E. Mazancová, S. Rusz, P. Kawulok, Arch. Civ. Mech. Eng. **12**, 312-317 (2012).
[26] S.S. Sohn, H. Song, B.C. Suh, J.C. Suh, J.H. Kwak, B.J. Lee, N.J. Kim, S. Lee, Acta Mater. **96**, 301-310 (2015).
[27] E. Mazancová, M. Cagala, B. Smetana, M. Žaludová, METAL 2013: 22nd International Conference on Metallurgy and Materials (2013).
[28] G. Niewielski, D. Kuc, J. Cebulski, S. Lalik, Archives of Materials Science and Engineering **47**, 1, 11-18 (2011).
[29] D. Janicki, M. Musztyfaga-Staszuk, Stroj. Vestn.J. Mech. E. **62** (6), 363-372 (2016).
[30] S. Lalik, D. Kuc, G. Niewielski, J. Cebulski, Hutnik – Wiadomości Hutniczne **8**, 641-645 (2011).
[31] B. Bhattacharya, A.S. Sharma, S. S. Hazra, R.K. Ray, Metall. Mater. Trans. A **40**, 1190-1202 (2009).
[32] L. Sozańska-Jędrasik, J. Mazurkiewicz, W. Borek, L.A. Dobrzański, Mater. Eng. **2**, 69-76 (2017).

[33] D. Pakuła, M. Staszuk, T. Tański, Mater. Technol. **50** (5), 755-759 (2016).

[34] M. Król, T. Tański, P. Snopiński, B. Tomiczek, J. Therm. Anal. Calorim. **127**, 1, 299-308 (2017), DOI 10.1007/s10973-016-5845-4.

[35] A. Zieliński, G. Golański, M. Sroka, Int. J. Pres. Ves. Pip. **152**, 1-6 (2017). DOI:10.1016/j.ijpvp.2017.03.002.

[36] M. Sroka, A. Zieliński, M. Dziuba-Kałuża, M. Kremzer, M. Macek, A. Jasiński, Metals-Basel **7** (3), 82 (2017), DOI:10.3390/met7030082.

[37] M. Sroka, A. Zieliński, A. Hernas, Z. Kania, R. Rozmus, T. Tański, A. Śliwa, Metalurgija **56** (3-4), 333-336 (2017).

[38] G. Golański, A. Zielińska-Lipiec, A. Zieliński, M. Sroka, J. Mater. Eng. Perform. **26** (3), 1101-1107 (2017). DOI:10.1007/s11665-017-2556-3

[39] A. Śliwa, W. Kwasny, M. Sroka, R. Dziwis, Metalurgija **56** (3-4), 422-424 (2017).

[40] Zieliński, M. Miczka, B. Boryczko, M. Sroka, Arch. Civ. Mech. Eng. (**4**), 813-824 (2016). DOI:10.1016/j.acme.2016.04.010.

[41] L.A. Dobrzanski, W. Borek, J. Mazurkiewicz, Materialwiss Werkst **47** (5-6) SI, 428-435 (2016).

[42] W. Borek, T. Tanski, Z. Jonsta, P. Jonsta, L. Cizek, Metal 2015: 24th International Conference on Metallurgy and Materials, 307-313 (2015).

[43] M. Król, T. Tański, W. Sitek, Mater. Sci. Eng. **95** A, 012006 (2015).

[44] S. Boncel, J. Gorka, M.S.P. Shaffer, K.K.K. Koziol, Mater Lett **116**, 53-56 (2014).